Automatic detection of microdots in the stromal layer of corneal images*

Jeffrey Wigdahl, Pedro Guimarães, Enea Poletti, and Alfredo Ruggeri

Abstract— **Microdots are bright, 1-2µm features of the cornea. It has not been proven what these dots represent, but they are thought to be remnants of apoptotic cell death, such as lipofuscin granules. Their presence has been shown to correlate with corneal aging and extended contact use, both of which are linked to oxygen deprivation in the cornea. Confocal images of the stroma show these microdots mixed with larger keratocyte cells. This paper presents a method for detecting microdots using a two-step filtering scheme that separates the keratocyte cells and the microdots. Keratocyte cell locations are then used to eliminate falsely detected microdots. Results are compared to ground truth based on a grading scale from 0-5. Two graders were given a set of 50 images to grade using a GUI that included sample images for each of the six grades. The two graders had a correlation of .88 with each other. The algorithm had a correlation of .88 with the average of graders and .85 with each of the graders individually.**

I. Introduction

Microdots are small (1-2µm), bright features that are found in the stromal layer of the cornea [1]. There is disagreement as to whether the dots are a normal feature of a healthy cornea [2,3], or only present due to oxygen deprivation or trauma to the cornea [4]. Studies have linked their presence and number to corneal aging and extended contact use [1,2,4]. There has not been a study to determine exactly what these microdots are made of, but it is widely thought that they consist of lipofuscin granules left behind by apoptotic death of the keratocyte cells that they are mixed with. Figure 1 shows examples of images containing microdots and keratocyte cells. These dots are highly reflective, and an increase in their numbers in the anterior stroma has been shown to produce higher levels of backscatter [5].

To our knowledge, there has not been any work in the automatic detection of microdots. This is likely due to the limited understanding of what they are and what their function is in a normal and abnormal cornea. Other features of the cornea have received much more attention, such as corneal nerve segmentation and analysis [6,7], which has been tied to peripheral neuropathy in diabetic patients.

*This research was made possible by a Marie Curie grant from the European Commission in the framework of the REVAMMAD ITN (Initial Training Research network), Project number 316990

J. Wigdahl, P. Guimarães, E. Poletti, and A. Ruggeri are with the Department of Information Engineering, University of Padova, Via Gradenigo 6/B, Padova, Italy

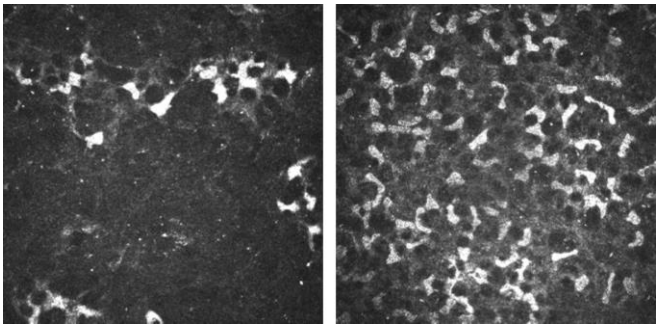

Figure 1: Example images of microdots mixed with keratocyte cells in confocal microscopy images of the stromal layer in the cornea.

In this paper, we present a method to detect microdots in confocal microscopy images of the stromal layer in the cornea. After preprocessing, a Laplacian of Gaussians (LoG) filter is used to detect possible microdot locations. Separately, the keratocyte cell network is segmented and used to determine falsely detected microdot locations. The proposed method is tested against grading's based on a 0-5 scale for the number of microdots.

II. Data Description

A total of 612 confocal microscopy images of the stromal layer were acquired from 102 volunteer subjects. The images were acquired using the Heidelberg Retina Tomograph (HRT-II) with the Rostock Cornea Module (Heidelberg Engineering GmbH, Heidelberg, German) at the Ophthalmology Department at Linköping University, Sweden. The instrument was outfitted with a 363/.95 NA immersion objective lens (Carl Zeiss SMT GmbH, Oberkochen, Germany) to cover a field of 400 x 400µm at 384 x 384 pixels. A subset of 50 images was randomly chosen for this study.

The 50 images were graded on a scale of 0-5 by two independent graders corresponding to the number of dots present in the image. Table 1 shows the grade breakdown for number of dots. The graders were provided with a graphical user interface that showed the image, filtered versions of the image, and reference images for each of the grade levels.

III. Methodology

This section describes the microdot detection algorithm. There are two main structures present in these images, microdots and keratocyte cells. They both appear as bright structures in the image, with their differences being in size

Table 1: Grading Criteria for Microdot images

Grade	Number of Dots
0	< 5
1	5 – 10
2	10 – 25
3	25 – 50
4	50 – 75
5	> 75

and shape. Part of our criteria for microdot detection states that microdots cannot form on top of keratocyte cells, allowing us to separate the two structures, forming the basis for our method.

All images undergo illumination and contrast correction before being processed. A standard morphological top-hat procedure is used which subtracts the morphological opening of image from the original [8].

A. Microdot enhancement filtering

The illumination corrected image is filtered with a LoG filter to enhance bright dots in the image. The Laplacian is a derivative filter that can detect fast changes in intensity (edges and dots), but is also very sensitive to noise. It is common to apply Gaussian smoothing before applying the Laplacian, and the combination of this process is the LoG filter [9]. Microdots can range in diameter from 1-5 pixels with a distinctly round shape. A 5x5 LoG filter was found to best enhance the microdots, along with a few of the edges of the keratocyte cells.

B. Keratocyte enhancement filtering

The same illumination corrected image is used for this step. To separate the microdots from the keratocyte cells, the dots are thought of as speckle noise, which can be adequately suppressed with the proper sized median filter [10]. This type of method has been used to denoise ultrasound images as well as radar signals [11,12]. For this work, a 7x7 median filter was found to maximally suppress the noise while maintaining the structure of the keratocyte cells.

C. Microdot detection

A simple thresholding is applied to both the filtered microdot and keratocyte images. Region properties are calculated in both binary images to exclude regions that do not fit the size and shape restrictions. For microdots, regions larger than 10 pixels would have their shape analyzed. If the regions had low eccentricity, they would be discarded. Keratocyte regions have a more irregular shape but should always appear much larger than the microdots. Regions smaller than 30 pixels were discarded leaving the final segmentation. Keratocyte regions are then dilated, and subtracting the keratocyte segmented images from the microdot candidate image, leaves only the detected microdot regions left. Eroding each region to a single pixel and summing the image gives the final microdot count. Figure 2 shows the workflow for the processing. The algorithm was evaluated using the Pearson product-moment correlation coefficient which measures the linear correlation between to variables.

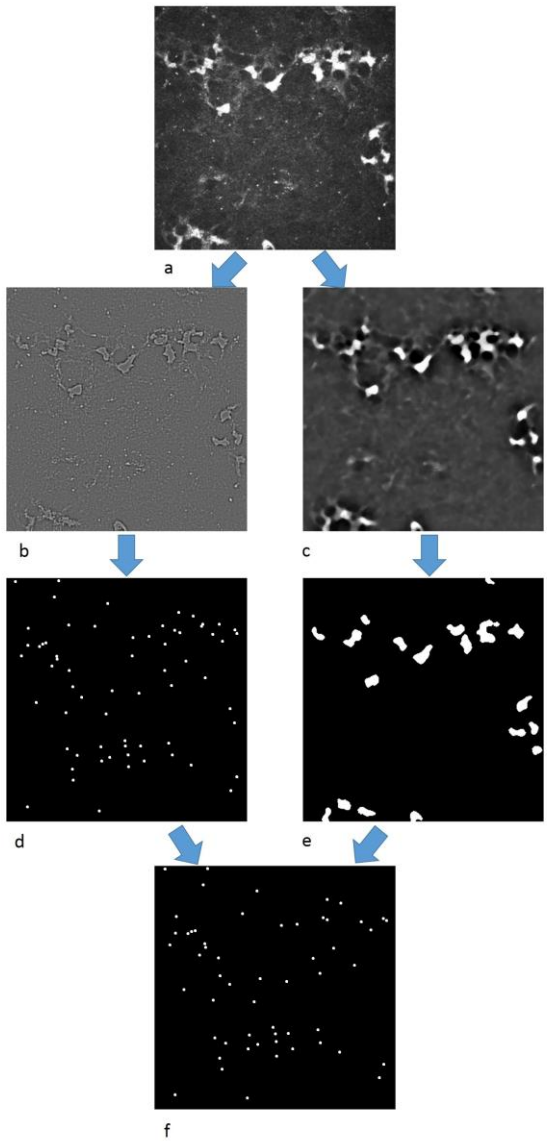

Figure 2: (a) The original image, (b) illumination corrected image filtered with the LoG filter, (c) the illumination corrected image filtered with the median filter, (d) detected microdot candidates, (e) segmented keratocyte cells, (f) final detection of microdots in the image after subtracting the keratocyte image from the microdot image.

IV. Results and Discussion

To evaluate the results of the algorithm, two graders graded the 50 image set on the 0 – 5 scale. The algorithm was then correlated to each of the individual graders as well as the average of their grades. The graders were given a

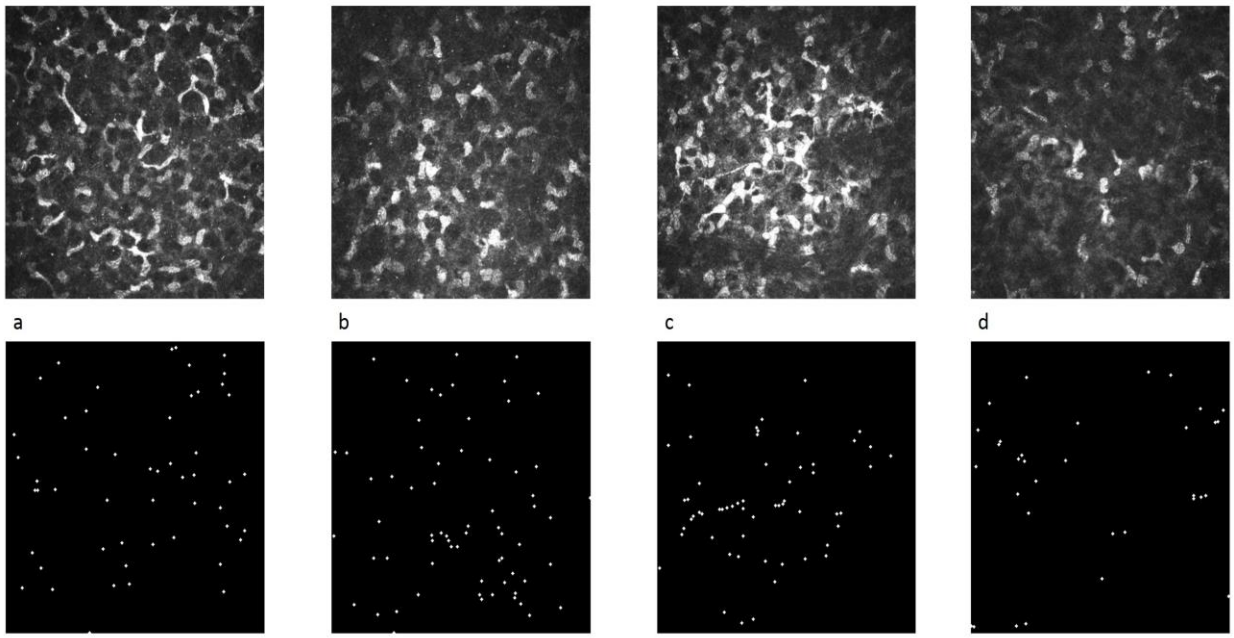

Figure 3: Each column shows the original image and the detected dots in the image. (a) This image had a manual and algorithm grade of 4. (b) This image had an average manual grade of 3.5 and an algorithm grade of 4. (c) Average manual grade of 1 and algorithm grade of 4. (d) Average manual grade of 0 and algorithm grade of 3.

GUI that displayed the image, along with filter options and example images for each grade. The two graders had a Pearson's linear correlation coefficient of .883. The algorithm had a correlation of .880 with the average of the two gradings and a correlation of .856 and .852 with the graders individually. The correlation between algorithm and graders shows that this detection method coincides with human visual perception. Human graders are unlikely to count the number of microdots in an image for several reasons. For one, there can be well over a hundred microdots present in an image. Most graders would not spend the time to count over 20, leaving grades 2-5 open to their interpretation. Two, images can appear to have what looks like a cloud of microdots, making the actual number in the cloud difficult to assess. Three, when keratocyte cells are just off of the imaging plane, it can make them look like clusters of microdots. Again, whether they are or not is open for interpretation. These reasons make the actual number of microdots in the image much less important and difficult to ground truth beyond the 0-5 scale.

The algorithm tends to have a higher grade than the manual gradings by a full grade, but the correlation shows that the grades can be linearly mapped to the correct ones in most cases. Figure 3 shows examples of the results achieved with the algorithm against both graders. Microdot detection areas are enlarged for visualization. Columns a and b show results that match the manual gradings. Columns c and d are the images with the highest grade differential. The higher grades come from the simple thresholding method for finding candidate microdots. There is an assumption that microdots will be present in the image, and when they are not, it is much more likely that false detection will occur. The other reason for higher grades is the shape of the keratocyte cells. They often taper at the ends to long points. These points are picked as microdot candidates, but are missed in the keratocyte segmentation process.

To again show that the algorithm agrees with the human perception of microdots, prior to grading the images, the graders were asked to rank the images from lowest to highest amount of microdots. The graders were provided a GUI that would display two images side by side. The grader would chose the image with more microdots and move on to the next pair of images. The GUI works to insure the lowest number of combinations necessary to complete the 50 image dataset. The graders were again able to rank the images with a high correlation of .90. The algorithm had a correlation of .84 with both of the individual graders and .85 with the average rank for each image.

The algorithm runs a single image using a single core MATLAB (The Mathworks Inc., Natick, MA) implementation in .18 +- .01s on an Intel Core i7-4770 CPU (Intel Corporation, Santa Clara, CA) at 3.4 GHz.

V. Conclusions

This paper presents a method for the automatic detection of microdots that correlates highly with manual gradings based on a 0 -5 scale and by ranking. More focus was put on making sure the algorithm correlated to human perception

rather than the exact number of dots in the image. The reason for this is the inexact nature of determining what is and is not a microdot. Also, when the microdots are on the smaller end of the micro spectrum, groups of microdots are difficult to separate. This is made especially difficult when the group of microdots is mixed between a large network of keratocytes. The low resolution can have the dots ranging down in size to a single pixel. The varying amount, size and shape of keratocyte cells make them difficult to capture using a single filter. Also, depending on where you are in the stroma, images may contain corneal nerves or endothelial cells.

Improvements to the algorithm would likely be seen by choosing a smarter thresholding scheme for candidate detection. This work, which is underway, includes feature selection and classification techniques to cut down the number of falsely detected microdots, and bring the algorithm in line with the manual grade levels. Also, the median filter used to detect the keratocyte cells could be replaced with an edge preserving filter that could help segment the cells, while still suppressing the noise.

This fully automatic algorithm can help ophthalmologist grade large datasets of microdot images in a short amount of time, with results that correlate highly to human graders. Portions of the code have also been ported to a GUI so that it can be run semi-automatically as well. The user is able to see the filtered images and likely microdot candidates, along with the original image to help graders make grading decisions. This will likely be important as more information becomes available on what these microdots are and what their role in the cornea is.

REFERENCES

[1] Hillenaar T, van Cleynenbreugel H, Remeijer L. How Normal Is the Transparent Cornea? Effects of Aging on Corneal Morphology. Ophthalmology. 2011

[2] R.G.A Faragher, B. Mulholland, S:J Tuft, S. Sandeman, P.T. Khaw, "*Aging and the Cornea*", Br J Ophthal, 81, (1997), pp. 814-817

[3] Efron N, Perez-Gomez I, Mutalib HA, Hollingsworth J. *Confocal microscopy of the normal human cornea*. Cont Lens Anterior Eye 2001;24:16 –24.

[4] Trittibach P, Cadez R, Eschmann R, et al. *Determination of microdot stromal degenerations within corneas of long-term contact lens wearers by confocal microscopy.* Eye Contact Lens 2004;30:127–31.

[5] Hillenaar T, Cals RH, Eilers PH, et al. *Normative database for corneal backscatter analysis by in vivo confocal microscopy*. Invest Ophthalmol Vis Sci 2011;52:7274–81.

[6] F. Scarpa, E. Grisan, A. Ruggeri, *Automatic recognition of corneal nerve structures in images from confocal microscopy,* Investigative Ophthalmology and Visual Science, 49(2008), pp. 4801-4807

[7] A. Ferreira, A.M. Morgado, J.S. Silva, *Corneal nerves segmentation and morphometric parameters quantification for early detection of diabetic neuropathy,* Proceedings of IFMBE MEDICON 2010, Greece, 29(2010) 264-267

[8] Soille Pierre. Morphological image analysis: principles and applications. Springer-Verlag New York, Inc. 2003

[9] M. Sonka, V. Hlavac, R. Boyle, Image Processing, Analysis and Machine Vision, Chapman & Hall, London, UK, NJ, 1993, pp. 193–242.

[10] T. Sun and Y. Neuvo, "Detail-preserving median based filters in image processing," Pattern Recognit. Lett., vol. 15, pp. 341–347, Apr. 1994.

[11] Czerwinski RN, Jones DL, O'Brien WD Jr. Ultrasound speckle reduction by directional median filtering. Proceedings of the 1995 IEEE International Conference on Image Processing 1995;1:358 – 361.

[12] M. Mansourpour, M.A. Rajabi, and J.A.R. Blais, "Effect and Performance of Speckle Noise Reduction Filter On Active RADAR and SAR Images," ISPRS Volume Number: XXXVI-1/W41, Ankara, Turkey, Feb 2006.